

Technological Development for Half-life Measurement of ^{146}Sm Nuclide

N. Kinoshita,^{*,†,a} T. Hashimoto,^a T. Nakanishi,^a A. Yokoyama,^a H. Amakawa,^b T. Mitsugashira,^c T. Ohtsuki,^d N. Takahashi,^e I. Ahmad,^f J. P. Greene,^f D. J. Henderson,^f C. L. Jiang,^f M. Notani,^f R. C. Pardo,^f N. Patel,^f K. E. Rehm,^f R. Scott,^f R. Vondrasek,^f L. Jisonna,^g P. Collon,^h D. Robertson,^h C. Schmitt,^h X. D. Tang,^h Y. Kashiv,ⁱ and M. Paulⁱ

^aGraduate School of Natural Science and Technology, Kanazawa University, Ishikawa 920-1192, Japan

^bOcean Research Institute, The University of Tokyo, Tokyo 164-8639, Japan

^cInstitute for Material Research, Tohoku University, Ibaraki 311-1313, Japan

^dGraduate School of Science, Tohoku University, Miyagi 982-0826, Japan

^eGraduate School of Science, Osaka University, Osaka 560-0043, Japan

^fPhysics Division, Argonne National Laboratory, Argonne, Illinois 60439, USA

^gDepartment of Physics and Astronomy, Northwestern University, Evanston, Illinois 60208-3112, USA

^hDepartment of Physics, University of Notre Dame, Notre Dame, Indiana 46556, USA

ⁱRacah Institute of Physics, Hebrew University, Jerusalem 91904, Israel

Received: December 7, 2006; In Final Form: January 3, 2007

Techniques for the measurement of the ^{146}Sm nuclide, which is known as an extinct nuclide on the present Earth, were developed in order to determine its half-life. The nuclide was produced in three reactions of $^{147}\text{Sm}(\gamma,n)^{146}\text{Sm}$, $^{147}\text{Sm}(n,2n)^{146}\text{Sm}$, and $^{147}\text{Sm}(p,2n)^{146}\text{Eu}(\rightarrow^{146}\text{Sm})$. The Sm fraction in the target was chromatographically purified to prepare α counting samples as hydroxide. The $^{146}\text{Sm}/^{147}\text{Sm}$ α -activity ratios in the samples were measured using a Si surface barrier detector. The $^{146}\text{Sm}^{22+}/^{152}\text{Sm}^{23+}$ and $^{147}\text{Sm}^{22+}/^{152}\text{Sm}^{23+}$ ratios were measured by accelerator mass spectrometry using the ECR-ATLAS-GFM system. The ^{146}Sm ions were distinguished clearly from the other ions such as the abundant isobar, ^{146}Nd in the samples.

1. Introduction

The α -emitting nuclide of ^{146}Sm is known as a p -process nuclide produced in supernova explosions. Recently, search for the nuclide is planned for various purposes in nuclear astrophysics, astrochemistry, etc. although it was not supposed to exist on the present Earth since its half-life is shorter by a factor of ~ 50 than the age of the Earth. The nuclide ^{146}Sm was first discovered by Dunlavey et al.¹ in an α -activated natural Nd sample using a nuclear emulsion. The half-life was estimated to be 5×10^7 y in the study according to the Geiger-Nuttall rule. After that, the half-life was measured to be $(7.4 \pm 1.5) \times 10^7$ y by Nurmia et al.² in 1964, and $(1.03 \pm 0.05) \times 10^8$ y by Friedman et al.³ in 1966. The currently adopted half-life of $(1.03 \pm 0.05) \times 10^8$ y was determined by Meissner et al.⁴ in 1987.

In determination of long half-lives, the half-life value is calculated usually from the relationship between radioactivity and the number of atoms. Many researchers often have difficulty in determining the number of atoms rather than in the radioactivity measurement. Nurmia et al.² and Meissner et al.⁴ estimated the number of ^{146}Sm atoms using γ activity of the parent nuclide of ^{146}Sm . For a direct measurement of atoms, Friedman et al.³ produced the ^{146}Sm atoms in $^{146}\text{Nd}(\alpha,xn)$ reactions, and the number of ^{146}Sm atoms was measured by a Thermal Ionization Mass Spectrometer (TIMS) after removal of the target material. The ^{146}Nd ions which are present in nature interfered with the ^{146}Sm detection in that case. In determination of the half-life of ^{146}Sm by mass spectrometry, the precision of the

measurements depends on the contamination by ^{146}Nd .

Recently Accelerator Mass Spectrometry (AMS) using a Gas-Filled Magnet (GFM) spectrograph has been well developed to attain excellent separation power, and used for the measurements of ^{36}Cl , ^{63}Ni , etc.^{5,6} However, the larger the atomic number of interest, the more difficult the separation of isobaric nuclides. In case nuclides with a large atomic number are measured with AMS, highly accelerated ions are required to separate isobaric nuclides. We carried out AMS measurements using the Argonne Tandem-Linac Accelerator System (ATLAS) of the Argonne National Laboratory for the reasons described above.

In the present study, we produced ^{146}Sm atoms using three nuclear reactions with Sm targets in order to prepare samples with different conditions in isotopic abundance and contamination by the other elements. Alpha spectrometry using a silicon semiconductor detector and mass spectrometry using an AMS technique were carried out to develop a method to determine the half-life of ^{146}Sm .

2. Calculation of the Half-life

The half-life of the ^{146}Sm nuclide is expressed referring to the naturally occurring nuclide of ^{147}Sm , which also emits an α -particle. The activities of ^{146}Sm and ^{147}Sm are described, respectively, as

$$A_{146} = \frac{\ln 2}{T_{146}} \times N_{146}, \quad (1)$$

and

$$A_{147} = \frac{\ln 2}{T_{147}} \times N_{147}, \quad (2)$$

*Corresponding author. E-mail: norikazu@post.kek.jp. Fax: +81-29-864-4051.

†Present address: Radiation Science Center, High Energy Accelerator Research Organization (KEK), 1-1 Oho, Tsukuba, Ibaraki 305-0801, Japan.

where T_{146} and T_{147} are the relevant half-lives, and N_{146} and N_{147} are the number of relevant atoms. Dividing eq 1 by eq 2 gives

$$T_{146} = \frac{A_{147}}{A_{146}} \times \frac{N_{146}}{N_{147}} T_{147}. \quad (3)$$

According to eq 3, the half-life of ^{146}Sm can be determined from the α -activity ratio by α spectrometry and the atomic ratio by mass spectrometry referring to the half-life of ^{147}Sm , $(1.17 \pm 0.02) \times 10^{11}$ y, which was determined previously.⁷

3. Experimental

3.1. Production of ^{146}Sm nuclide.

3.1.1. (γ, n) reaction. Bremsstrahlung radiation (maximum energy, 50 MeV; flux, $\sim 10^{13}$ eq.q. s^{-1}) was introduced to a target of 93% enriched ^{147}Sm oxide and the irradiation was performed for ~ 100 hours at the Laboratory of Nuclear Science, Tohoku University to produce ^{146}Sm atoms by the $^{147}\text{Sm}(\gamma, n)^{146}\text{Sm}$ reaction. The yield of ^{146}Sm was estimated to be ~ 120 mb eq.q. $^{-1}$ by using the PICA3/GEM code.⁸ After the irradiation, the Sm target was dissolved in hydrochloric acid. The solution adjusted to the acidity of ~ 0.5 M HCl was let pass through a strong cation-exchange resin column (4.6 mm ϕ \times 250 mm) which was conditioned with NH_4Cl solution and kept at 80 °C in a column oven. Then distilled water was let pass through the column to settle the Sm ions in the resin. Finally, 0.3 M 2-hydroxyisobutyric acid (α -HIBA) solution which contained 3 g of NaCl per 500 mL in concentration and was adjusted to pH 4.2 with NaOH was let pass through the column to elute the Sm ions chromatographically prior to the Pm ions produced in the (γ, p) reaction. The Sm fraction was acidified with HCl, and a Fe carrier was added. After the Sm was recovered with $\text{Fe}(\text{OH})_3$, the precipitate was dissolved in 12 M HCl solution and the solution was let pass through a Dowex 1X8 anion-exchange column to remove the Fe ions.

3.1.2. ($p, 2n$) reaction. A 21-MeV proton beam (~ 1 μA) was delivered to a 96% enriched ^{147}Sm oxide at Research Center for Nuclear Physics, Osaka University. The irradiation continued for 12 hours to produce the EC/ β^+ -decaying nuclide of ^{146}Eu ($T_{1/2} = 4.61$ d) by the $^{147}\text{Sm}(p, 2n)$ reaction. The cross section of the reaction was estimated to be 1.1 b according to a calculation by the ALICE code⁹ and Reference 10. Europium isotopes were isolated from the target material by the same cation-exchange chromatography as mentioned in the preceding paragraph, and let stand for ~ 2 months to grow the ^{146}Sm daughter. Then, the Sm isotopes in the Eu fraction were separated using cation-exchange chromatography to remove by-products such as a weak α emitting nuclide, ^{147}Eu ($T_{1/2} = 24.1$ d) which could be produced by the $^{148}\text{Sm}(p, 2n)$ reaction.

3.1.3. ($n, 2n$) reaction. Fast neutrons of $\sim 3 \times 10^{19}$ cm^{-2} in fluence in the energy range of 6–10 MeV were bombarded to a 96% enriched ^{147}Sm oxide in a Japan Material Testing Reactor at the Institute for Materials Research, Tohoku University to produce ^{146}Sm atoms by the $^{147}\text{Sm}(n, 2n)$ reaction. The target was dissolved in HCl, and then a concentration of HCl was adjusted to 0.25 M. The solution was let pass through an Ln resin column (0.75 cm ϕ \times 4.5 cm, 2 mL) supplied by Eichrom Technologies, Inc. The Sm isotopes were recovered with 11 mL of 0.4 M HCl. This chromatographic procedure was repeated 5 times to improve the purity of the Sm fraction.

3.2. Alpha spectrometry. Each of the Sm samples of 20–100 μg was precipitated with ammonia water and collected on a Fuji Film Teflon membrane filter (pore size: 0.2 μm) attached to a plastic filter holder with a 4.9 cm^2 filtering area to prepare a counting sample. The α activity on the filter was measured using an EG & G Ortec OctetTM PC α -spectrometer equipped with a silicon surface-barrier detector of 450 mm^2 for the active

area. A counting sample was placed in a vacuum ($< \sim 4$ Pa) chamber of the spectrometer with a solid angle of $\sim 20\%$ of 4π geometry. The typical energy resolution of the α -spectrometer was ~ 50 keV (FWHM) for α -particles from ^{147}Sm , and the typical background of the spectrometer was ~ 5 cpd in the peak region of ^{147}Sm (2.235 MeV).

3.3. Accelerator mass spectrometry. The Sm samples on filters that were subjected to α spectrometry were, at a later stage, dissolved with HCl and the ^{147}Sm contents of the samples were determined with a SEIKO SPQ-9000 ICP-MS. A known amount of each of the samples was diluted with an HCl solution containing a known amount of natural Sm (100 mg) to approximately 10^{-8} of $^{146}\text{Sm}/^{147}\text{Sm}$ atomic ratio to prepare a sample of volume and atomic ratio suitable for the AMS measurement. The HCl concentration of the solution was adjusted to 0.25 M and the solution was passed through an Ln resin column (0.75 cm ϕ \times 4.5 cm, 2 mL). Neodymium isotopes which interfered with the ^{146}Sm measurement in mass spectrometry were eluted with 20 mL of highly purified 0.25 M HCl solution which was prepared by diluting TAMAPURE-AA-10 reagent supplied by Tama Chemicals Co. Ltd. with Milli-Q water. Subsequently, Sm isotopes were eluted with 10 mL of purified 0.5 M HCl solution as described above. This separation procedure was repeated twice, and the Sm sample was precipitated with TAMAPURE-AA-10 ammonia water. The precipitate was heated at 450 °C for 7 hours to convert hydroxide to oxide. The oxide was mixed well with twice its weight of Zr metal powder, and put into a Ta boat. Electric current of approximately 70 A was applied to the boat in a vacuum chamber ($< \sim 10^{-6}$ Torr) to reduce the oxide to metal because Sm ions are produced from a metal form rather than an oxide form in the ECR plasma chamber as an AMS ion source.

Measurements of ^{146}Sm with AMS using an Electron Cyclotron Resonance Ion Source (ECR-IS) were performed at Argonne National Laboratory (ANL). The ATLAS system¹¹ was entirely tuned with a $^{80}\text{Kr}^{2+}$ pilot beam, which has a mass-to-charge ratio close to that of $^{146}\text{Sm}^{22+}$, prior to the AMS measurement of $^{146}\text{Sm}^{22+}$. The difference in the mass-to-charge ratio is $\delta(m/q)/(m/q) = 4.6 \times 10^{-3}$. The ions produced in ECR-IS were extracted from the ion source with a voltage of 200 kV, and analyzed through a bending trajectory with three analyzing magnets to select ions of interest, and then accelerated by three kinds of superconductor linear accelerators of Positive Ion Injector (PII), BOOSTER Linac, and ATLAS Linac. Finally, the ions passed through a GFM entrance, which consists of Mylar of 1.4 μm in thickness and entered a GFM spectrograph. The arrangement of the Faraday cup, GFM, ionization chamber, Position-Sensitive Parallel-Grid Avalanche Counter (PGAC) is shown in Figure 1. The $^{146}\text{Sm}^{22+}$ ion was selected for acceleration because of its suitable mass-to-charge ratio which is not interfered with strongly by other ions except for ^{146}Nd . The $^{146}\text{Sm}^{22+}$ ions were accelerated to 840 MeV, and introduced to the GFM spectrograph^{12,13} filled with 10-Torr N_2 gas and subjected to 14 kG of magnetic field to separate the intense stable isobar ^{146}Nd from ^{146}Sm . The $^{146}\text{Sm}^{22+}$ and $^{146}\text{Nd}^{22+}$ ions slowed down in the GFM, and trajectories of the ions were deflected by the magnetic field. The position of each ion at the focal plane was monitored with the PGAC. In order to decrease the counting rate of the ionization chamber, blocking shield was inserted at the focal plane to block other ions accelerated together with $^{146}\text{Sm}^{22+}$ and $^{146}\text{Nd}^{22+}$. After the ions passed through the PGAC, multiple energy-losses along the ion path, $\Delta E_1 - \Delta E_5$ and ΔE_{total} , were measured in an ionization chamber. The signal of Time Of Flight (TOF) was also measured as the time difference between the PGAC signal and RF master signal of the accelerator. The $^{152}\text{Sm}^{23+}$ ions which have a mass-to-charge ratio close to that of the $^{146}\text{Sm}^{22+}$ ion ($\delta(m/q)/(m/q) = 4.2 \times 10^{-3}$) were counted by a Faraday cup set up in the GFM beamline. The measurements with the cup were per-

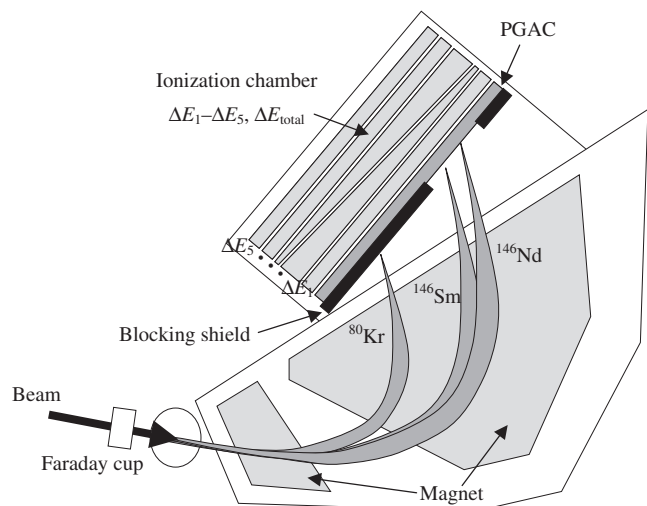


Figure 1. Arrangement of Faraday cup, GFM, and Ionization-Chamber/PGAC. Ions were analyzed in GFM, positions of the ions at the focal plane were monitored with PGAC, and multiple energy losses (ΔE_1 – ΔE_5 and ΔE_{total}) were measured with an ionization chamber. The $^{147}\text{Sm}^{22+}$ and $^{152}\text{Sm}^{23+}$ ions were measured with the Faraday cup. The Faraday cup was removed to count the $^{146}\text{Sm}^{22+}$ and $^{146}\text{Nd}^{22+}$ ions with PGAC-IC system.

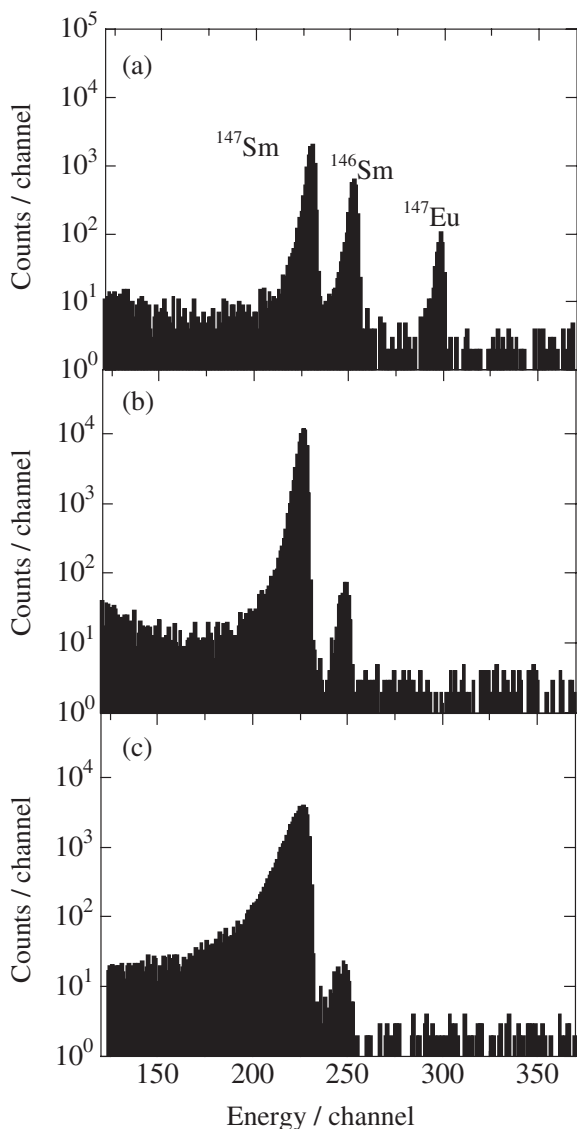


Figure 2. Alpha spectra of the Sm samples from (a) proton-activation, (b) neutron-activation, and (c) bremsstrahlung-activation. Thicknesses of the $\text{Sm}(\text{OH})_3$ counting samples are $\sim 10 \mu\text{g}/\text{cm}^2$ for proton-activation (a), $\sim 15 \mu\text{g}/\text{cm}^2$ for neutron-activation (b), and $\sim 25 \mu\text{g}/\text{cm}^2$ for bremsstrahlung-activation (c).

formed in between the measurements of the ^{146}Sm ions. Ions of $^{147}\text{Sm}^{22+}$ were also counted with the Faraday cup to derive the $^{146}\text{Sm}/^{147}\text{Sm}$ atomic ratio through the ratios of $^{146}\text{Sm}^{22+}/^{152}\text{Sm}^{23+}$ and $^{147}\text{Sm}^{22+}/^{152}\text{Sm}^{23+}$. In the measurements with the Faraday cup, the other ions of contaminants are negligible compared with the Sm ions.

4. Results and Discussion

Alpha spectra of the Sm isotopes which were produced in three reactions measured with a silicon surface barrier detector, are shown in Figure 2. The $^{146}\text{Sm}/^{147}\text{Sm}$ α -activity ratio was determined from α -peak counts of these nuclides. The FWHM and FWTM of approximately 50 keV and 90 keV, respectively, for the proton-activated sample, 60 keV and 130 keV, respectively, for the neutron-activated sample, and 100 keV and 230 keV, respectively, for the bremsstrahlung-activated sample were observed for the ^{147}Sm α peak. The precision of the $^{146}\text{Sm}/^{147}\text{Sm}$ α -activity ratio was hardly influenced by the correction for the tailing of α peaks under the above conditions of FWHM and FWTM.

Two-dimensional plots of position along the focal plane vs. ΔE_1 and those gated by TOF are shown in Figure 3. The two-dimensional plot for the blank $^{\text{nat}}\text{Sm}$ sample, which was not activated, is shown in Figure 4 for comparison. Two components are clearly distinguished in Figure 3, showing each of the components has its characteristic trajectory and velocity in GFM. One component was identified to be from ^{146}Sm ions from the extrapolation of the measured energy losses and positions for the ions of $^{147}\text{Sm}^{22+}$, $^{152}\text{Sm}^{22+}$, and $^{154}\text{Sm}^{22+}$. The other component is interpreted as resulting from $^{146}\text{Nd}^{22+}$ ions, which have the same m/q ratio as the $^{146}\text{Sm}^{22+}$ ion.

The separation between ^{146}Sm and ^{146}Nd ions at the focal plane arises mainly from a different mean charge of the ions in GFM. The mean charge of the ions in material, \bar{q} , can be calculated with the following equation:¹⁴

$$\bar{q} = Z[1 - A(Z)\exp(-0.879V_R)], \quad (4)$$

with $A(Z) = 1.035 - 0.4\exp(-0.16Z)$ and $V_R = V/(V_0 Z^{0.65})$, where Z is the atomic number, V is the velocity of the projectile, and V_0 is $2.188 \times 10^8 \text{ cm/s}$. The mean charge of the ^{146}Sm ions is larger by ~ 1 than that of ^{146}Nd ions. Thus, the ^{146}Sm events should appear at a lower channel in the position spectrum than that of the ^{146}Nd events. It agrees with the assignment described above.

The different energy losses between ^{146}Sm and ^{146}Nd seen in Figure 3 result from the combination of the different incident energy to the ΔE_1 detector, i.e., the different energy losses between ^{146}Sm and ^{146}Nd ions in the GFM before entering into the ΔE_1 , and those in the ΔE_1 detector. The energy loss of the ^{146}Sm ion in the GFM is larger than that of ^{146}Nd , which leads to the higher incident energy of ^{146}Nd to the ΔE_1 detector than that of ^{146}Sm . The higher energy ^{146}Nd ions may lose a larger amount of energy in the ΔE_1 detector than that of ^{146}Sm for the relevant incident energies, which is consistent with the observed energy losses in Figure 3. In addition, the higher-energy ^{146}Nd ions in the GFM than ^{146}Sm allow us to separate those nuclides in the TOF spectrum; the higher energy ^{146}Nd ions should appear at lower channels in TOF than ^{146}Sm , which agrees with the experimental results.

We measured the activated Sm samples prior to the blank $^{\text{nat}}\text{Sm}$ sample in order to investigate the optimum condition for ^{146}Sm measurement. Thus, the ^{146}Sm events observed in Figure 4 using the blank $^{\text{nat}}\text{Sm}$ sample are attributed to the memory effect. These events were found to be so low that background events could be neglected in the measurements of the activated Sm samples. The separation between the ^{146}Nd and ^{146}Sm ions using the GFM technique was found successful, even in case

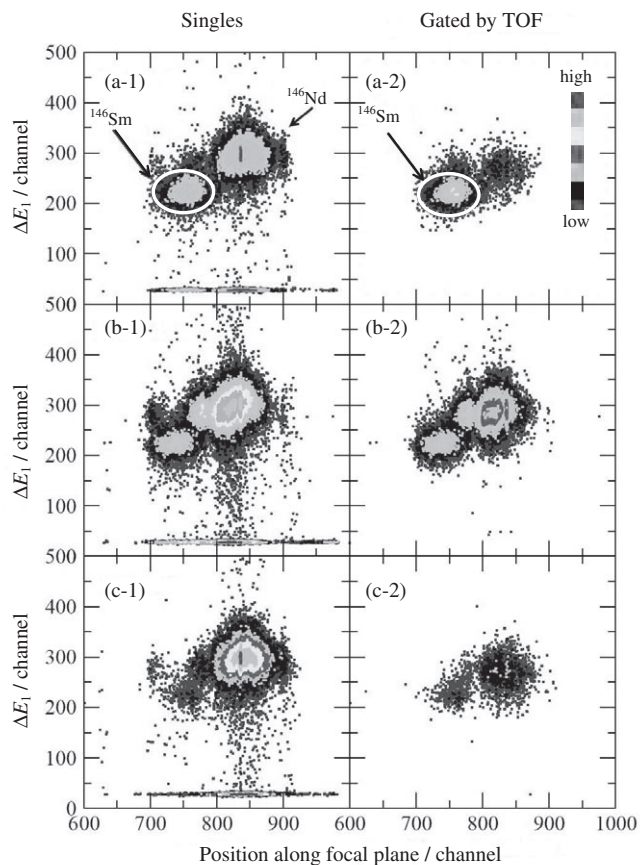


Figure 3. Two-dimensional plot of position along focal plane vs. ΔE_1 in AMS. The figures of (a-1) and (a-2) are for proton-activated sample, (b-1) and (b-2) for neutron-activated sample, and (c-1) and (c-2) for bremsstrahlung-activated sample. Those of (a-1), (b-1), and (c-1) show raw data, while (a-2), (b-2), and (c-2) are the data gated by TOF. The numbers of $^{152}\text{Sm}^{23+}$ ions were deduced to be 1.1×10^{12} for proton-activated sample (a), 8.6×10^{11} for neutron-activated sample (b), and 8.6×10^{11} for bremsstrahlung-activated sample (c) according to ion-counting with a Faraday cup at intervals between the measurements of ^{146}Sm .

the ^{146}Nd ions were more intense than the ^{146}Sm ions by a factor of 10–100. In the AMS, however, further normalization is required to correct for differences in experimental conditions of $^{146}\text{Sm}^{22+}$, $^{147}\text{Sm}^{22+}$, and $^{152}\text{Sm}^{23+}$ measurements for the determination of the half-life of ^{146}Sm .

5. Summary

In order to develop techniques for the measurement of the half-life of ^{146}Sm , nuclides were produced in $^{147}\text{Sm}(p,2n)^{146}\text{Eu}(\rightarrow ^{146}\text{Sm})$, $^{147}\text{Sm}(n,2n)^{146}\text{Sm}$, and $^{147}\text{Sm}(\gamma,n)^{146}\text{Sm}$ reactions. Alpha counting samples were prepared as Sm hydroxide to measure the $^{146}\text{Sm}/^{147}\text{Sm}$ α -activity ratios with a Si semiconductor detector. The Sm samples for AMS were prepared through chemical procedures. The $^{146}\text{Sm}^{22+}/^{152}\text{Sm}^{23+}$ and $^{147}\text{Sm}^{22+}/^{152}\text{Sm}^{23+}$ ratios were measured using the ECR-ATLAS-GFM system of ANL to determine the $^{146}\text{Sm}/^{147}\text{Sm}$ atomic ratio. The $^{146}\text{Sm}^{22+}$ ions were successfully distinguished from the $^{146}\text{Nd}^{22+}$ ions by AMS. Further normalization is, however, required to correct for differences in experimental conditions of the measurements of $^{146}\text{Sm}^{22+}$, $^{147}\text{Sm}^{22+}$, and $^{152}\text{Sm}^{23+}$ for the determination of the half-life of ^{146}Sm .

Acknowledgements. We would like to thank the staff of the Laboratory of Nuclear Science, Tohoku University for the bremsstrahlung irradiation, the Institute for Materials Research, Tohoku University for the neutron irradiation, and the Research Center of Nuclear Physics, Osaka University for the proton

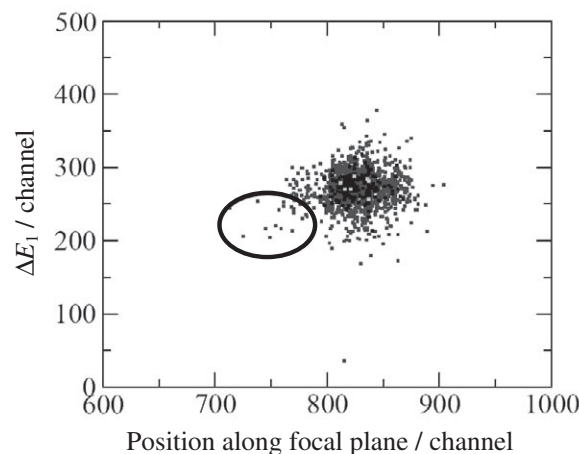


Figure 4. Two-dimensional plot of position along focal plane vs. ΔE_1 for the non-activated Sm sample gated by TOF. The ^{146}Sm events in a circle might be attributed to the memory effect. The number of $^{152}\text{Sm}^{23+}$ ions was deduced to be 3.4×10^{13} in the same way as described in the caption of Figure 3.

irradiation. We also wish to acknowledge the assistance of the members of the ATLAS facility, Argonne National Laboratory for utilization of the accelerator mass spectrometry.

References

- (1) D. C. Dunlavey and G. T. Seaborg, *Phys. Rev.* **92**, 206 (1953).
- (2) M. Nurmia, G. Graeffe, K. Valli, and J. Aaltonen, *Ann. Acad. Sci. Fenn. A VI*, **148**, (1964).
- (3) A. M. Friedman, J. Milsted, D. Metta, D. Henderson, J. Lerner, A. L. Harkness, and D. J. Rokop, *Radiochim. Acta* **5**, 192, (1966).
- (4) F. Meissner, W. D. Schmidt-Ott, and L. Ziegeler, *Z. Phys. A* **327**, 171 (1987).
- (5) S. Hatori, H. Nawata, M. Ohseki, H. Matsuzaki, T. Misawa, and K. Kobayashi, *Nucl. Instrum. Methods Phys. Res. B* **172**, 211 (2000).
- (6) H. Nassar, M. Paul, I. Ahmad, D. Berkovits, M. Bettan, P. Collon, S. Dababneh, S. Ghelberg, J. P. Greene, A. Heger, M. Heil, D. J. Henderson, C. L. Jiang, F. Käppler, H. Koivisto, S. O'Brien, R. C. Pardo, N. Patronis, T. Pennington, R. Plag, K. E. Rehm, R. Reifarth, R. Scott, S. Sinha, X. Tang, and R. Vondrasek, *Phys. Rev. Lett.* **94**, 092504 (2005).
- (7) N. Kinoshita, A. Yokoyama, and T. Nakanishi, *J. Nucl. Radiochem. Sci.* **4**, 5 (2003).
- (8) T. Sato, K. Shin, S. Ban, Y. Namito, H. Nakamura, and H. Hirayama, *Nucl. Instrum. Methods Phys. Res. A* **437**, 471 (1999).
- (9) M. Blann and H. K. Vonach, *Phys. Rev. C* **23**, 1427 (1983).
- (10) K. Katoh, H. Miyahara, N. Marnada, N. Ueda, K. Ikeda, K. Fujiki, H. Haba, I. Nishinaka, K. Tsukada, Y. Nagame, M. Asai, and S. Ichikawa, *J. Nucl. Sci. Technol.* **39**, 329 (2002).
- (11) W. Kutschera, I. Ahmad, P. J. Billquist, B. G. Glagola, R. C. Pardo, M. Paul, K. E. Rehm, and J. L. Yntema, *Nucl. Instrum. Methods Phys. Res.* **B42**, 101 (1989).
- (12) M. Paul, *Nucl. Instrum. Methods Phys. Res.* **B52**, 315 (1990).
- (13) M. Paul, B. G. Glagola, W. Henning, J. G. Keller, W. Kutschera, Z. Liu, K. E. Rehm, R. Schneck, and R. H. Siemssen, *Nucl. Instrum. Methods Phys. Res.* **A277**, 418 (1989).
- (14) F. Hubert, A. Fleury, R. Bimbot, and D. Gardes, *Ann. Phys. Fr.* **5** (Suppl.), 1 (1980).